Patterning nonflat substrates with a low pressure, room temperature, imprint lithography process

Matthew Colburn
Texas Materials Institute, The University of Texas at Austin, Austin, Texas 78727

Annette Grot
Agilent Technologies Laboratory, Agilent Technologies, Palo Alto, California 94304

Byung Jin Choi
Texas Materials Institute, The University of Texas at Austin, Austin, Texas 78727

Marie Amistoso
Agilent Technologies Laboratory, Agilent Technologies, Palo Alto, California 94304

Todd Bailey, S. V. Sreenivasan, John G. Ekerdt, and C. Grant Willson[a)]
Texas Materials Institute, The University of Texas at Austin, Austin, Texas 78727

(Received 21 June 2001; accepted 17 September 2001)

Step and flash imprint lithography (SFIL) is a technique that has the potential to replace photolithography for patterning resist with *sub*-100 nm features. SFIL is a low cost, high throughput alternative to conventional photolithography for high-resolution patterning. It is a molding process in which the topography of a template defines the patterns created on a substrate. The ultimate resolution of replication by imprint lithography is unknown but, to date, it has only been limited by the size of the structures that can be created on the template. It is entirely possible to faithfully replicate structures with minimum features of a few hundred angströms. SFIL utilizes a low-viscosity, photosensitive silylated solution that exhibits high etch contrast with respect to organic films in O_2 reactive ion etching. In this article we describe the SFIL process, the development of a multilayer etch scheme that produces 6:1 aspect ratio features with 60 nm linewidths, a method for patterning high-aspect-ratio features over topography, and a metal lift-off process. A micropolarizer array consisting of orthogonal 100 nm titanium lines and spaces fabricated using this metal lift-off technique is reported. [DOI: 10.1116/1.1417543]

I. BACKGROUND

Will optical lithography ever reach its limit? A combination of improvements in optics, further reduction in wavelength, and introduction of more complex masks and processes will surely enable printing features smaller than 100 nm. Unfortunately, the cost of optical exposure tools is increasing exponentially.[1] The Semiconductor Industry Association (SIA) Roadmap lists several alternative ''next generation lithography'' (NGL) techniques based on ionizing radiation:
x ray, extreme ultraviolet (EUV), electron projection lithography (EPL), and direct-write electron beam. Each has its advantages and disadvantages, but all are expensive. We seek in inexpensive method for pattern generation capable of sub-100 nm resolution on substrates, silicon or otherwise. If such a method is to be significantly cheaper than proposed NGLs, it must, by necessity, be very different from those now contemplated.

Photolithographic resolution follows the well-known relationship[2]

$$R = \frac{k\lambda}{\mathrm{NA}}, \tag{1}$$

where k is a system dependent parameter, which includes resist material contrast, λ is the wavelength of the light, and NA is the numerical aperture of the lens. Imprint lithography has several important advantages over conventional optical lithography and NGLs. The parameters in Eq. (1) are not relevant to imprint lithography because the technology is not limited by optical diffraction. The resolution of imprint techniques in the sub-100 nm regime is well documented[3–8] and appears to be currently limited by the resolution of structures that can be generated in the template or mold. Imprint templates are typically fabricated using imaging tools such as electron beam writers that provide high resolution but lack the throughput required for mass production. Imprint lithography therefore takes advantage of the resolution offered by e-beam technology without compromising throughput.

There are many imprint lithography techniques, all variations on a common theme. The basic premise is that a template or mold with a prefabricated topography is pressed into a displaceable material. That material takes on the shape of the master pattern defined in the template, and the shaped material is cured into a solid. The process is by nature a contact patterning process that transfers patterns without scaling, and so there are common challenges to all of these imprint techniques, the foremost being the dependence of this technology on 1× imprint master resolution, and defect production and propagation.

a)Corresponding author; electronic mail: willson@che.utexas.edu

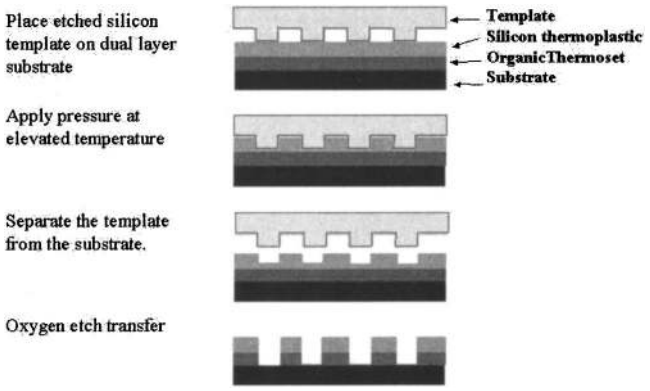

FIG. 1. Step and squish imprint lithography. An organic thermoset is spin coated onto a substrate. A silylated thermoplastic is spin coated onto the coated substrate. A template that is patterned with a topography is brought into contact with this film stack. Pressure greater than 0.3 MPa is applied at temperatures above the glass transition temperature of the silylated thermoplastic resulting in its displacement. This pattern is then transferred to the underlying layer by a short halogen RIE followed by an O_2 RIE.

Researches systematically studied imprint lithography techniques in the 1990s.[3–8] The research is divided into two camps, one camp prefers imprinting into a thermoplastic or thermoset polymer, and the other imprinting into an UV light-curable material. Chou *et al.*,[5] Schultz *et al.*,[9] Scheer *et al.*,[10] and Jaszewski *et al.*[8] followed the same basic technology: a polymer heated above its glass transition temperature (T_g) is imprinted with a mold. The system is cooled to below the T_g of the polymer while the mold is in contact, thus fixing the shape of the imprint. This process has demonstrated remarkable resolution with features as small as 10 nm.[5]

Early in our research program, we investigated the prospect of imprinting a silylated thermoplastic at elevated temperatures and pressures.[3] Our goal was to generate a bilayer structure analogous to that produced by bilayer or trilayer lithographic processes.[11] This process, called "step and squish imprint lithography," is shown in Fig. 1. Some results from this compression molding study are described in a previous publication;[3] they illustrate a serious problem with this approach. Imprinting with varying pattern density results in incomplete displacement of the thermoplastic even at elevated temperature and high pressure for long periods of time. A simple depiction of this result is illustrated in Fig. 2. Partial pattern transfer, failure to displace material completely, release difficulties, and harsh process conditions limit the potential of this approach. Scheer *et al.*[10] also have documented these problems in compression molding of PMMA derivatives. More important, we decided that the use of high temperatures and high pressures would severely limit our ability to achieve the layer-to-layer alignment required for microelectronic device fabrication.

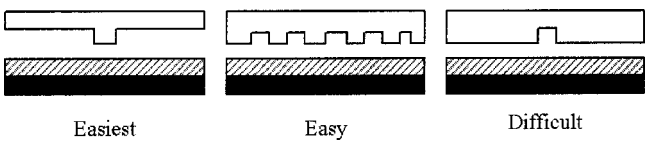

FIG. 2. Pattern density effects found during SSIL. Periodic patterns and isolated protruding features are replicated relatively easily. Isolated recessed patterns are difficult to imprint successfully.

The second route to imprint lithography relies on curing a low-viscosity, photosensitive material with ultraviolet light. This method has been used in the production of optical disks.[12] Philips Research has demonstrated a photopolymer process of this sort which produces high-resolution polymer features.[7] In this process, a liquid acrylate formulation was photopolymerized in a glass template to generate the required topographical features. While the Philips process shows promise for creating high-resolution images, it did not produce high-aspect-ratio images, and the patterned acrylate polymers lack the etch resistance required for semiconductor manufacturing. Because of our experience and that of others, we choose to refocus our efforts on a different technique that we call step and flash imprint lithography.

II. PROCESS DESCRIPTION

Step and flash imprint lithography (SFIL) is a low pressure, room temperature technique that utilizes a rigid quartz template. The SFIL process has been given in detail previously.[3] Briefly, a substrate is coated with an organic polanarization layer, known as te "transfer layer," and brought into close proximity to a low surface energy template bearing low aspect-ratio topography. A low viscosity UV-sensitive organosilicon solution, called the etch barrier, is deposited between the template and the coated substrate. The template is brought into contact with the substrate using minimal pressure to trap the photopolymerizable etch barrier solution in the topography of the template. Then, the template is illuminated with UV through its backside thereby crosslinking the organosilicon solution at room temperature. The low viscosity acrylic based photopolymer formulation, the details of which were reported previously,[3] requires a dose of approximately 20 mJ/cm^2, which is comparable to that of chemically amplified resists used in high volume manufacturing. The template is then separated from the substrate leaving a polymer replica of its relief image on the substrate. This patterned substrate is first etched with a short halogen breakthrough reactive ion etch (RIE) followed by an O_2 RIE to form a high-resolution, high-aspect-ratio feature.

The SFIL development program has proceeded down two parallel paths. A SFIL stepper was developed to conduct multiple imprints on a 200 mm wafer and it is dedicated to a statistical defect study. At the same time, a collaboration with Agilent Technologies was established to develop the etch transfer process.[4] Work at Agilent Technologies was performed using a roller-press imprint system.[4] The two versions of the SFIL process are shown in Fig. 3.

The SFIL process has also been adapted for patterning over nonflat surfaces. First, a layer of poly(methylmethacrylate) (PMMA) was spin coated on substrates bearing a topography and hard baked at 200 °C for 2–4 min. A UV crosslinkable organic film was coated on the substrate and cured through the backside of a *featureless* (flat) template.

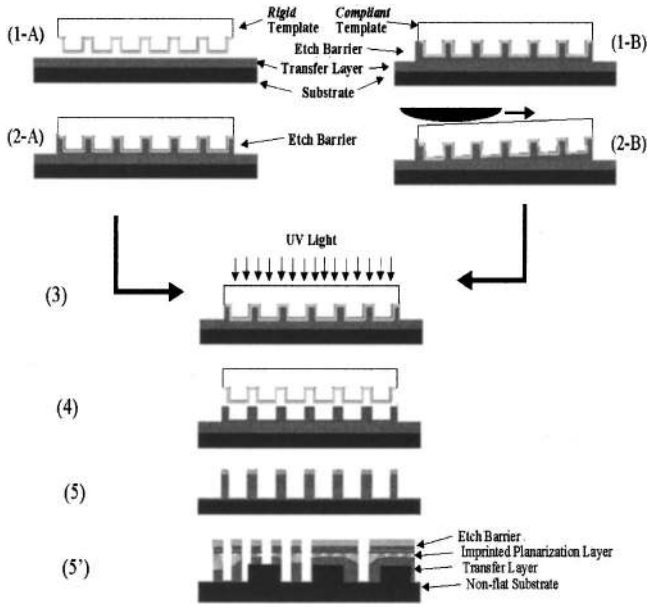

FIG. 3. Step and flash imprint lithography process using (A) a rigid template with the SFIL stepper and (B) a compliant template with Agilent imprint equipment. Step 5′ shows the result of patterning over topography.

This process planarizes the substrate [Figs. 3(1B)–(3–5)′]. The planarized substrate is then patterned with the SFIL process using a template. Finally, this relief structure is etch transferred through the imprinted planarization layer, the transfer layer. The resulting structure is shown in Fig. 3(5′). PMMA was chosen for this set of experiments because an overetch provides compatibility with additive metallization.

The viscosity of the photopolymerizable etch barrier solution plays a critical role in the SFIL process. An analytical model was given in detail previously that describes the relationship of the pressure (P) required to displace a liquid of viscosity (μ) and surface tension (γ) as two plates approach each other at a velocity ($2v$) while separated by a distance ($2H$).[13] It is shown below in more detail. Equation (2) refers to the case of a fixed volume (K) being displaced from the gap ($2H$) between the substrate and template. It also includes the effect of capillary pressure for the fluid meniscus with a radius (H_{curv}):[13]

$$P=\left(P_{\mathrm{atm}}-\frac{\gamma}{H_{\mathrm{curv}}}\right)+\frac{3\mu v K}{8\pi H^4}. \tag{2}$$

Further evaluation of the above relationship shows that a liquid having a viscosity of 1 cP can be displaced down to a thickness of less than 100 nm in 1 s with 14 N applied to a template having a radius of 1 cm.[14] In comparison, a fluid with viscosity of 100 cP takes over 100 s under identical conditions. It should be noted that this analysis is a worst-case scenario of imprinting a featureless template and that polymers heated above their T_g have viscosities greater than 100 cP.

The surface energy of the etch barrier must be designed to support filling of the capillary between the template and substrate. Following UV curing the etch barrier must adhere to the coated substrate and release completely and reliably from the surface-treated template. The treated template has a surface energy of approximately 21 dynes/cm.[3] Untreated templates exhibit a surface energy of ~50 dynes/cm.[3] Work on adhesion calculations shows that the release will occur preferentially at the etch barrier/treated template interface; our experiments are fully consistent with this prediction.[3] Further improvement in the surface treatment protocol decreased the posttreatment template surface energy to 14 dynes/cm, hence improving the release properties.[15]

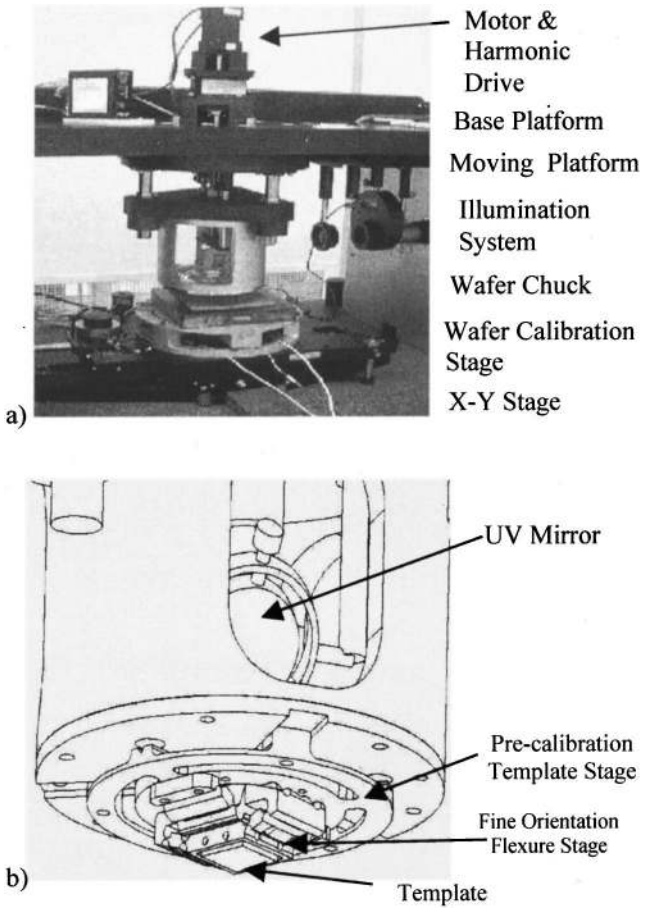

FIG. 4. SFIL stepper developed at the University of Texas at Austin.

III. SFIL STEPPER DESIGN

A multi-imprint step and flash lithography machine that can perform repeated imprints on 200 mm wafers was developed for defect analysis, and it is shown in Fig. 4. This machine can imprint high-resolution (sub-100 nm) features from quartz templates using a step and repeat process. The major machine components include the following: (i) a microresolution Z stage that controls the average distance between the template and substrate and the imprinting force; (ii) an automated $X-Y$ stage for step and repeat positioning; (iii) a pre-calibration stage that enables parallel alignment between the template and substrate by compensating for orientation errors introduced during template installation; (iv) a fine-orientation flexure stage that provides highly accurate,

passive parallel alignment of the template and wafer to the order of tens of nanometers across an inch;[16] (v) a flexure-based wafer calibration stage that orients the top of the wafer surface parallel to the plane of the XY stage; (vi) an exposure source that is used to cure the etch barrier; (vii) an automated fluid delivery system that accurately dispenses known amounts of the liquid etch barrier; and (viii) load cells that provide both imprinting and separation force data.

The multi-imprint apparatus is currently configured to handle 2.54 cm $\times$ 2.54 cm (6.45 cm^2) templates. It is used to produce more than 20 imprints on 200 mm wafers for defect studies. The installation of the template and loading and unloading of the wafer are performed manually. The printing operations, including $X-Y$ positioning of the wafer, dispensing of the etch barrier liquid, translation of the template to close the gap between the template and wafer, UV curing of the etch barrier, and controlled separation are all automated. These unit processes are controlled by a LabVIEW® interface. Detailed information about the major subcomponents of the system is available in publications by this group.[16]

Figure 5(a) shows two flat surfaces representing a template and a substrate. Proper alignment between these two flats ideally leads to a perfectly uniform surface contact between them. Such alignment can be accomplished with one translation motion (z displacement) and two tilting motions (α and β) between two flats. Figure 5(b) shows an ideal kinematic stage composed of perfect rigid bodies and joints. Nonideal behavior including distributed structural compliance, backlash and stiction in joints, etc., is neglected. Ideal kinematic stages provide insight into the geometry and force transmission at the template/substrate interface. This insight is then extended to the design of distributed flexure stages with selectively compliant and stiff directions.[16]

Connection from the base platform to the moving platform is via a combination of a revolute (R) joint, a prismatic (P) joint, and a ball (B) joint. The ideal kinematic stage has several practical limitations with respect to the SFIL process. The presence of sliding contacts in joints can cause wear, generate undesirable particles, and lead to stiction that makes precise motion control difficult. Clearances in joints can lead to reduced repeatability in the motion of the mechanism. Flexures generate motion by elastic deformation and can avoid all the problems associated with joints. Also, provided the elastic and fatigue limits are not exceeded, flexures can provide extremely repeatable motion and long life for the stage. Flexure stages are therefore becoming more common in the precision engineering industry.[16,17]

The three necessary motions were identified above (z, α, β). In ideal situations, the translation motions of the template in X and Y should be reserved for layer-to-layer alignment. Figure 5(c) shows a coupled effect between the orientation tilt and undesirable translation motions. When a tilting axis does not exist on the surface of the template, a side drift, d_s, of the template is given by $d_s = h \sin\theta \cong h\theta$, where h is the offset of the tilting axis from the surface and θ is the tilting angle in radians. As an example, when $h = 3$ mm and $\theta = 0.0001$ rad, d_s is 300 nm. Such excessive template side motion must be avoided because during the separation process after the etch barrier has already been UV exposed, excessive side motions would destroy transferred images.

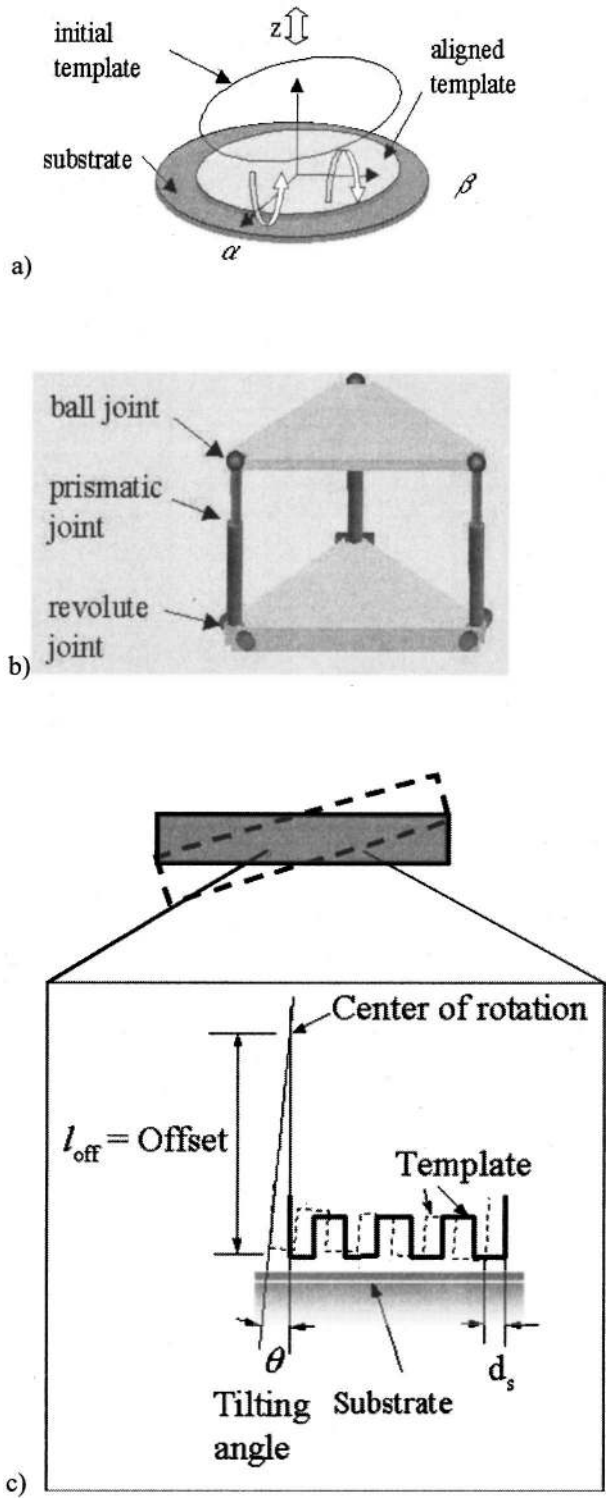

FIG. 5. (a) Desired orientation alignment motions; (b) ideal kinematic model; (c) possible offset, d_s, caused by a tilt axis offset a distance, h, from the template surface.

Multiple imprints are performed by moving a 200 mm wafer to various $X-Y$ positions while holding the template

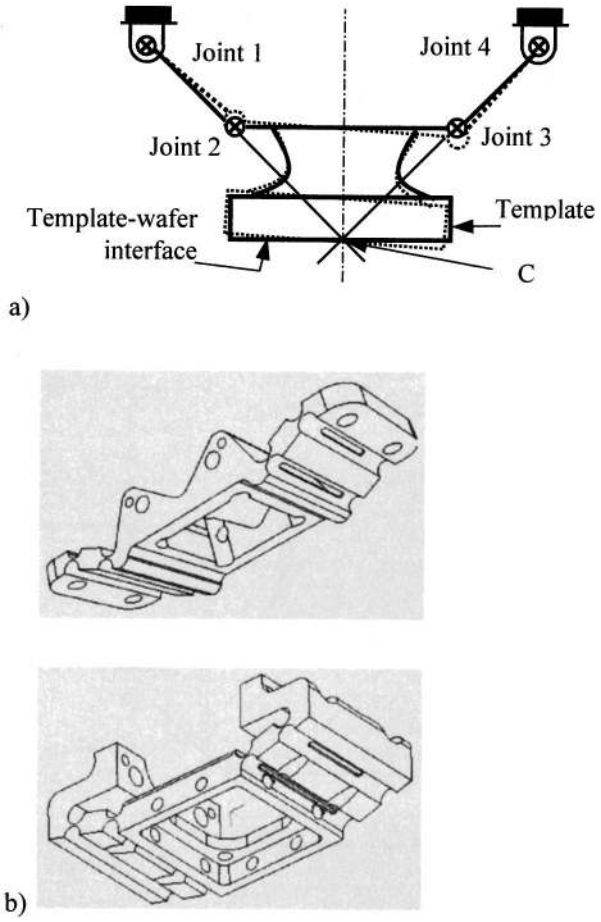

FIG. 6. (a) Template stage design showing one tilting axis and (b) implementation for two tilting axes.

stationary. For the multi-imprint process, it is necessary to have the compliant flexure affixed to the template since a rigid template and compliant wafer stage can lead to an unstable configuration for off-center imprinting.[16] Hence an orientation stage design that can tilt the template about the two "remote axes" that lie on the template–wafer interface [one of them denoted as "C" in Fig. 6(a)] was developed and is described in detail elsewhere.[16] The stage is constructed from two flexures that are mounted orthogonal to each other in order to generate two tilting motions.

IV. EXPERIMENTAL DESCRIPTION

A. Templates

Master templates for the University of Texas (UT) SFIL collaboration were prepared on Si or GaAs substrates that had been patterned with a JEOL electron beam lithography tool. These were used to generate daughter templates by replicating the relief structures in an UV curable polymer, J-91,[18] on flexible polycarbonate. These daughter templates were then coated with 10 nm of a fluorinated film that acts as a low surface energy release layer. This film was deposited in a C_3F_8 radio frequency (rf) plasma deposition chamber at 66 Pa and 100 W. The water contact angle on the deposited fluorinated film was greater than 90° after deposition.

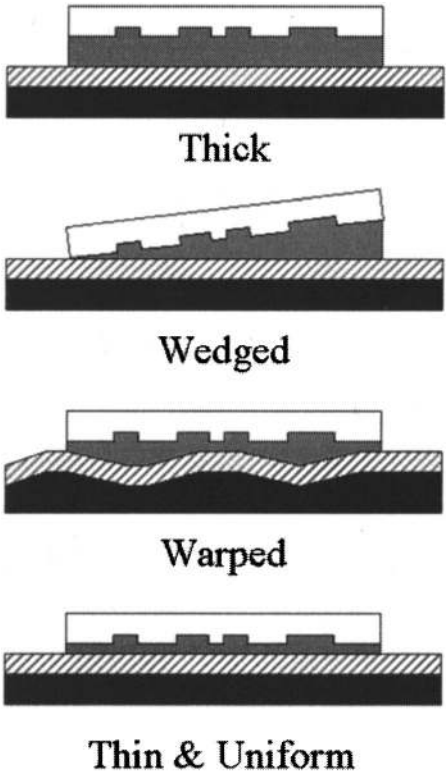

FIG. 7. Several types of base layers. Only the thin uniform base layer allows successful etch transfer over the entire imprint field.

For base layer characterization and etch work performed at the University of Texas at Austin, a quartz template generated by conventional phase-shift reticle fabrication techniques was used. These templates were treated with (tridecafluoro-1,1,2,2-tetrahydrooctyl)trichlorosilane (Gelest) as a release agent. Contact angles greater than 90° persisted for over 30+ imprints and several aggressive cleanings. The surface energy of these templates was 21 dynes/cm even after 3 months of use.[3] We continue to study the durability of the release treatment as well as alternative methods of deposition.[13]

B. Base layer studies with the SFIL stepper

The undisplaced etch barrier that remains after imprinting is termed the "base layer." Several types of base layers are possible and they are shown in Fig. 7. Only a thin and uniform base layer is useful for controllable etch transfer. In order to achieve a thin and uniform base layer with a rigid template, coplanarity between the entire substrate and the template must be ensured by performing a calibration procedure with the SFIL stepper. A test wafer coated with the same transfer layer thickness as the wafers to be imprinted is used in this procedure. The template is lowered an identical amount in three corners of the wafer located near each of the three force transducers on the wafer stage and the force is recorded. If the forces are unequal, the system's orientation is corrected by manipulating three micrometers attached to the flexure-based wafer calibration stage until the forces are equal.

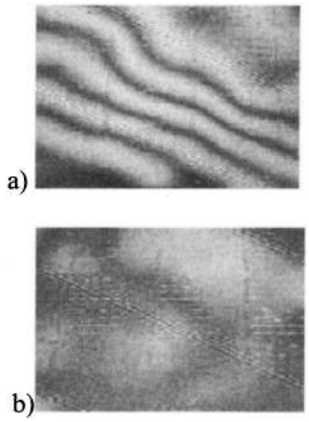

FIG. 8. Fizeau fringe patterns observed through the backside of the template when monochromatic light of wavelength 546.1 nm is used; (a) before calibration and (b) after calibration.

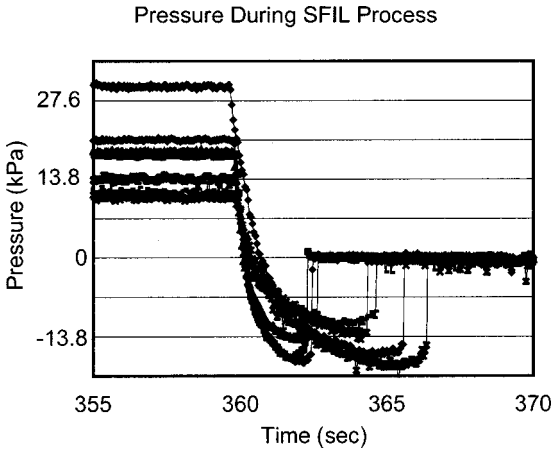

FIG. 9. Pressures monitored during the imprint and separation steps of SFIL. The stepper includes three force transducers capable of monitoring both the imprint pressure and separation pressure.

Once the measured forces are balanced, the orientation of the template to the wafer surface is inspected. The template is lowered into the center of the wafer until small pressure, typically 3–4 kPa, is generated. Three micrometers attached to the flexure calibration stage were adjusted to orient the template while observing Fizeau interference fringes across the entire 2.54 cm × 2.54 cm (6.45 cm^2) template. When the number of fringes drops below one, as in Fig. 8(b), the variation in the gap is less than 150 nm across the template, well within the capture range of the fine orientation template stage shown in Fig. 6(b). Once calibrated, it is possible to imprint at more than 25 locations across the 200 mm wafer with a 6.45 cm^2 template using the stepper's automated control system. The etch barrier is cured while under approximately 14 kPa of imprint pressure.

C. Fluid delivery

Fluid delivery is a critical unit operation in SFIL. It affects both the imprint uniformity and the processing time. A volume of etch barrier between 0.1 and 1.0 μl is dropped onto a wafer prior to the template being brought into proximity of the substrate. Nonsymmetric pressure applied to the template generated by asymmetric fluid deposition (i.e., a single drop placed off center) generates rotation in the template about the tilt axis causing an edge of the template to prematurely touch the template, making capillary action the predominant means by which to fill the gap near that edge. This change in gap height dramatically increases the fill time as predicted by Eq. (3), the Washburn equation, since the rate of fill is proportional to the gap height. In the Washburn equation, L is the position of the meniscus along the length of the capillary, H is the gap between the template and the substrate, and t_{fill} is the time required to fill to position L.[13] Asymmetric fluid deposition also induces nonuniformity in the base layer:

$$\frac{dx}{dt}\alpha\frac{H}{x}\Rightarrow t_{\text{fill}}\alpha\frac{L^2}{H}. \tag{3}$$

Due to symmetry of the system and the fluid dynamics governing the behavior of fluid displacement in capillaries, it is desirable to dispense the fluid in a pattern that is continuous and that causes a zero effective moment about the tilt axes of the fine orientation template stage. By using symmetric patterns, such as X, W, N or $+$, it has been determined experimentally that the fluid fills the gap more evenly and more quickly by minimizing any rotation of the template about the tilt axis of the fine orientation flexure.

The UT SFIL stepper allows simultaneous application of imprint pressure and UV exposure. At Agilent, on the other hand, the imprint pressure and exposure are performed sequentially in two distinct systems. Since the compliant template used at Agilent is not a rigid optical flat (such as the one used at UT), deformation is inherently required to maintain uniform contact with the etch barrier. When applied pressure is removed during transfer of the template/substrate stack to the exposure system, the fluid must be sufficiently viscous to maintain the strain in the compliant template.

As a result, the etch barrier formulation used at Agilent was primarily 95% (w/w) acryloxypropylmethsiloxane-dimethylsiloxane (Gelest) to 5% (w/w) free radical generator. This mixture was diluted either 1:7 or 1:15 in cyclohexanone depending on the template feature depth and topography duty cycle. This solution was spin coated for 60 s at 4000+ rpm onto a substrate generating a thin film on the order of 100–500 nm. The cyclohexanone evaporated, leaving an etch barrier film with viscosity of less than 120 cP. The volume of fluid remaining on the substrate was approximately equal to the volume of the template topography. The film is then imprinted using the two-stage Agilent imprint equipment. Both the imprint pressure and separation pressure can be measured on the SFIL stepper (shown in Fig. 9) whereas the imprint pressure at Agilent cannot be measured since the required instrumentation is not available on the imprint system.

D. Reactive ion etch studies

The SFIL process produces low-aspect-ratio relief structures that are amplified to obtain high-aspect-ratio structures by an O_2 RIE in the transfer layer. A base layer of undisplaced etch barrier is always present even if perfect orientation alignment has been achieved. Fluid dynamics predict that it is impossible to completely eliminate the base layer in finite time under finite pressure. Therefore a halogen etch is required to eliminate the silylated base layer prior to the O_2 RIE that transfers the pattern into the transfer layer.

A Materials Research Corporation (MRC) parallel plate, capacitively coupled rf reactive ion etcher with a 15.24 cm diam grounded electrode, a 15.24 cm driven lower electrode, and a 5.08 cm electrode gap was used for all of the etch work described in this article. The substrate rested on a 0.635 cm thick, 15.24 cm diam quartz plate. The etch rates were measured using *in situ* HeNe interferometry and were validated by both pre-etch and postetch two-angle ellipsometry and profilometry measurements.

The etch conditions for O_2 RIE were 40 sccm O_2, and 200 V at 20 mTorr. This etch was approximately 80% anisotropic, thus providing the degree of undercut necessary for subsequent additive metallization. The halogen etch conditions were 56 sccm CHF_3, 12.5 sccm He, and 450 V at 6 mTorr. Lowering the pressure from 20 to 6 mTorr reduced the undercut. For sub-100 nm features, 1 sccm O_2 was added to the halogen etch.

A study was carried out to determine the weight percent of silicon that must be incorporated into the etch barrier in order to achieve an etch rate ratio greater than 10 between the etch barrier and the transfer layer. Formulations with varying silicon contents were prepared by mixing cyclohexyl acrylate (Aldrich) and (3-acryloxypropyl)-tris(trimethylsiloxy)silane (Gelest) with a constant 5% (w/w) 1,3-bis(3-methacryloxypropyl) tetramethyldisiloxane (Gelest). The mixtures ranged from 95% (w/w) cyclohexyl acrylate to 95% (w/w) (3-acryloxypropyl)-tris(trimethylsiloxy)silane with the constant 5% (w/w) 1,3-bis(3-methacryloxypropyl) tetramethyldisiloxane. A 1:1 mixture of bis(2,4,6-trimethylbenzoyl)-phenylphosphineoxide (Irgacure 819, Ciba) and 1-benzoyl-1-hydroxycycloxhexane (Irgacure 184, Ciba) was added to the above solution at 3% (w/w) to initiate free radical polymerization upon UV illumination. For ~30% (w/w) silicon samples, acryloxypropylmethsiloxane-dimethylsiloxane low molecular weight polymer (Gelest) was used.

Two organic films were used as model transfer layer materials during the RIE studies: polystyrene and PMMA. A 10% (w/w) solution of polystyrene (50 000 molecular weight) in toluene was spun at 4000 rpm for 60 s and postapply baked at 90 °C for 90 s. A 10% (w/w) solution of PMMA (496 000 molecular weight) in chlorobenzene was spun at 4000–6000 rpm for 60 s depending on the thickness desired and then hard baked at 200 °C for 4 min under vacuum.

A preliminary RIE process based on the RIE collaboration with Agilent Technologies was developed at The University of Texas at Austin for use with the quartz template process shown in Fig. 3(A) steps 1–5. This work was performed on an Oxford Instruments Plasmatek μ80 parallel plate, capacitively coupled rf reactive ion etcher that was donated by 3M. It has a 15.24 cm diam lower driven electrode and a 30.48 cm diam grounded upper electrode. The gap between the electrodes is 5.08 cm. The O_2 RIT conditions were 10 sccm O_2, and 215 W at 10 mTorr. Two halogen RIE conditions were utilized: 28 sccm CF_4, 8 sccm He, and 1 sccm O_2 with 215 W at 10 mTorr for the images in Fig. 18, and 28 sccm CF_4, 5 sccm O_2 with 215 W at 10 mTorr for the images in Fig. 17(c).

For these initial etch transfer investigations, a transfer layer of PMMA 100 nm thick was spin coated and postapplication baked at 200 °C for 2+ h. The etch barrier formulation was 47% (3-acryloxypropyl)-tris(trimethylsiloxy)silane, 47% butylacylate, 2.3% 1,3-bis(3-methacryloxypropyl) tetramethyldisiloxane, 1.85% bis(2,4,6-trimethylbenzoyl)-phenylphosphineoxide, and 1.85% 1-benzoyl-1-hydroxycycloxhexane, by weight.

V. RESULTS

Previously we predicted that SFIL low viscosity solutions can be displaced to less than 100 nm with as little as 14 kPa in a matter of seconds.[13] The thickness of the undisplaced etch barrier (base layer) measured less than 55 nm with a flexible template, and in many cases even less using spin coating and the drop method described above. Figure 10(a) shows a scanning electron microscopy (SEM) image of such a base layer. The base layer for this sample ranges from <10 to 80 nm in thickness measured across a 2.54 cm × 2.54 cm patterned region using two-angle ellipsometry [shown in Fig. 10(b)]. This is quite extraordinary considering the templates utilized ~1% pattern coverage meaning that 99% of the solution must be displaced. Figure 10(c) is a SEM image of a 138 nm base layer achieved using a rigid transparent template that extended across 2.54 cm of the imprint field. The rigid template has the added benefit of low imprint deformation that is required for actual device fabrication and the possibility of layer-to-layer alignment.

These base layers readily allow the etch process to amplify the low-aspect-ratio relief into high-aspect-ratio features. During development of the etch transfer process, we varied the composition of the etch barrier formulations from almost entirely organic to 30% (w/w) silicon. The etch rate was measured in both halogen and O_2 RIE using *in situ* HeNe interferometry and the initial and final thicknesses were corroborated by both two-angle ellipsometry and profilometry. The etch was conducted with 40 sccm O_2 at 2.67 Pa and applied rf voltage of 250 V (33 W). The O_2 etch selectivity starts at 1:1 and increases to 60:1 for 30% (w/w) silicon formulations. As the silicon weight percent increases beyond 11% (w/w) the desired etch selectivity of 10:1 is achieved as shown in Fig. 11. Therefore, the etch barrier solutions currently used contain a minimum of 11% (w/w) silicon. Additionally, it was found that lowering the pressure

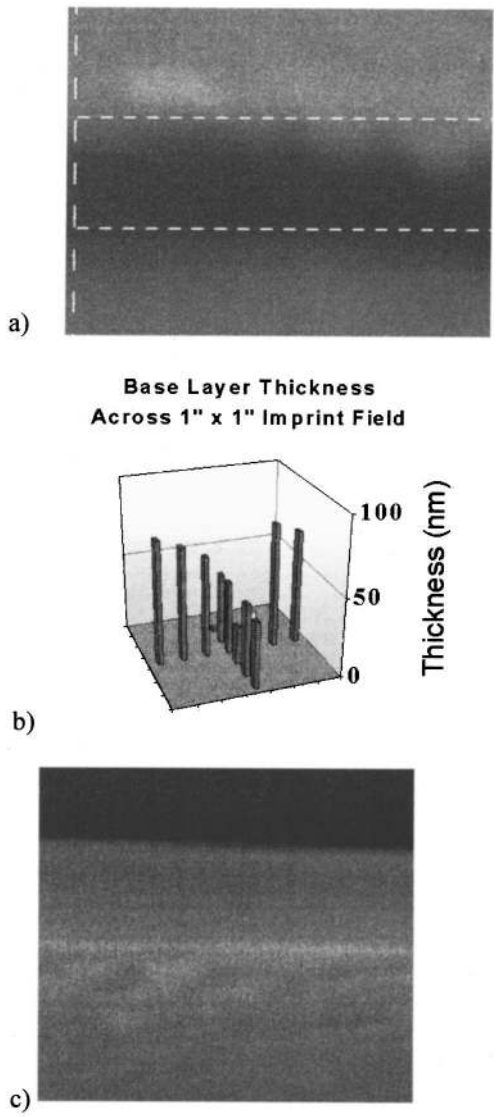

FIG. 10. (a) SEM image of an approximately 55 nm base layer after imprinting a polycarbonate template with the Agilent imprint equipment. (b) Base layer across a 2.54 cm × 2.54 cm patterned region measured with ellipsometry for the Agilent experiment. (c) 38 nm base layer imprinted with a quartz template in the SFIL stepper at the University of Texas at Austin. The arrows in (a) and (c) indicate the silylated base layer thickness.

from 2.67 to 0.8 Pa during the O_2 etch increased the side wall angle (reduced the undercut).

With the proper etch conditions for transfer identified, the resolution of the process was studied. An etch stop experiment was conducted in which the O_2 RIE was stopped after only partially penetrating the transfer layer. Using a wafer with 80 nm features replicated on 1.1 μm of hard-baked PMMA, the O_2 RIE was halted after penetrating 300 nm into the PMMA transfer layer. The sample was characterized by SEM [shown in Fig. 12(a)]. After determining that the features could structurally withstand both high-aspect ratios and the etch conditions, another section of the same wafer was etched until the endpoint was determined by HeNe interferometry. This sample was also characterized by SEM and is shown in Fig. 12(b). These features have a remarkable aspect

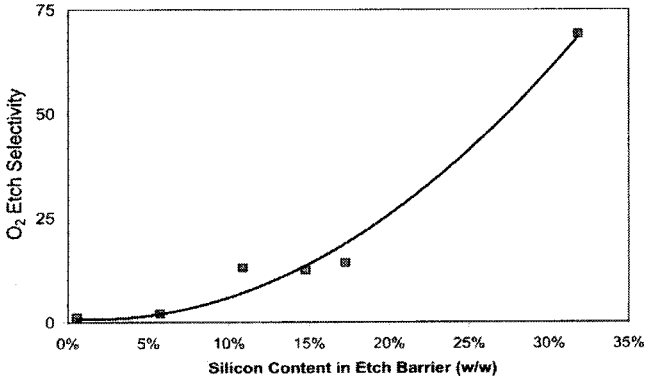

FIG. 11. Reactive ion etch selectivity between the etch barrier and a polystyrene film during O_2 etch as it increases with an increase in silicon content.

ratio of 14:1 and demonstrate one benefit of SFIL's silylated multilayer scheme over other imprint techniques.

A second high-resolution template was created using a single path e-beam exposure in 100 nm of PMMA. The result was a master with 60 nm features etched 50 nm deep. A daughter template was replicated from this master onto a polycarbonate sheet. Wafers were coated with 300 nm of hard baked PMMA and patterned with these 60 nm features. A short 20 s halogen breakthrough etch followed by an O_2 transfer etch generated 60 nm features with 6:1 aspect ratios and the slight undercut needed for lift-off metallization. These features are shown in Fig. 13.

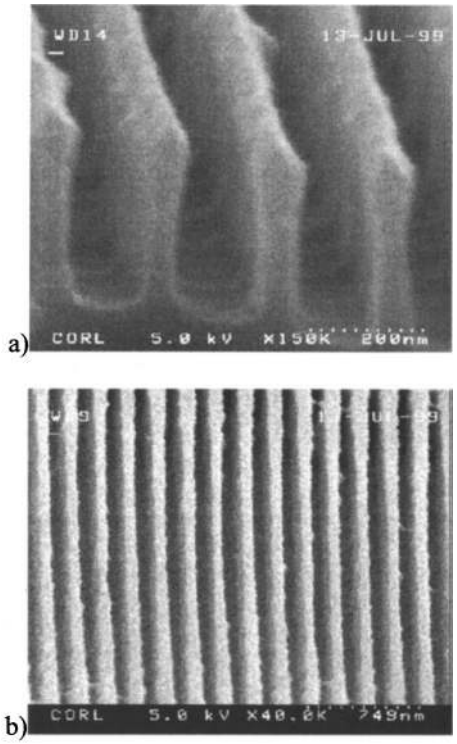

FIG. 12. (a) 80 nm wide lines on a 200 nm pitch partially transferred through a 1.1 μm layer of PMMA in an etch-stop experiment. (b) Top-down view of these features transferred through the entire PMMA layer.

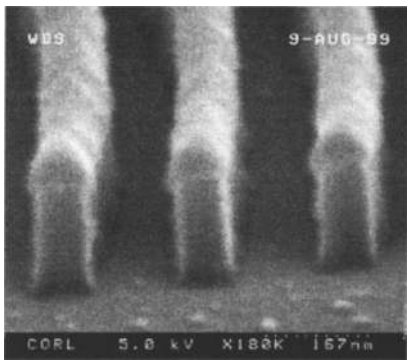

FIG. 13. 60 nm features with 6:1 aspect ratios.

On a separate sample, Ti was deposited on 100 nm structures at a rate of 2.5 nm/s in a metal evaporator. The Ti metal line remained after acetone liftoff in an ultrasonic bath. Figure 14(b) shows 100 nm metal lines patterned with a 100 nm line/space (L/S) template. The height of the metal lines is 50 nm. The aspect ratio of the patterns plays a critical role in determining the performance for many optical devices.

A high-resolution template with an array of orthogonal 100 nm L/S was replicated, etch transferred, and used to perform metal liftoff as described above, except in this case 100 nm of Ti was deposited rather than 50 nm as in Fig. 14(b). The result was an alternating array of orthogonal micropolarizers, shown in the optical micrograph of Fig. 15. Alternating arrays pass one polarization of light. Figure 15(a) was taken with nonpolarized light. There is uniform transmission in all the patterned areas. Figure 15(b) was taken with polarized light and this results in alternating light and dark regions. The polarization ratio was measured between 5:1 and 10:1 but could be improved by redesigning the support struts built into the micropolarizer array. Figure 15(c) is a top down micrograph of these 100 nm L/S.

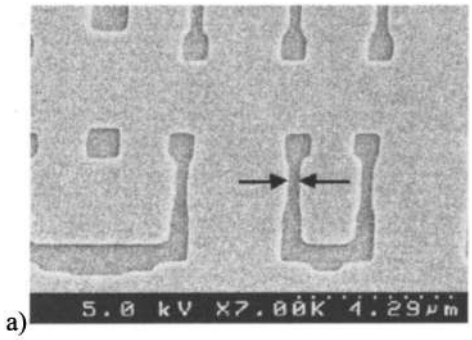

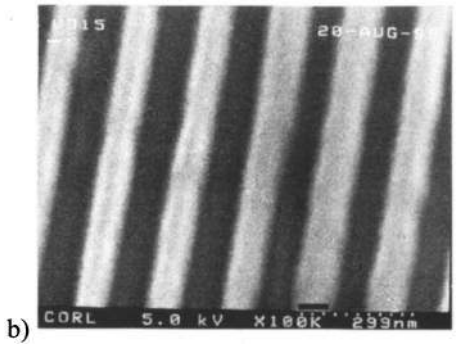

FIG. 14. (a) Ti liftoff of the 300 nm feature; (b) 100 nm Ti metal lines created using metal liftoff and SFIL.

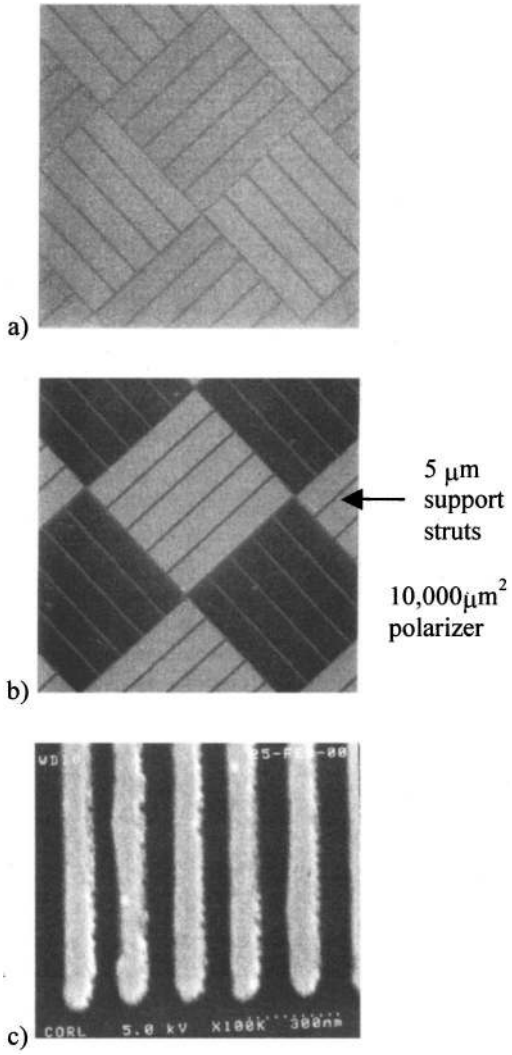

FIG. 15. Optical micrograph of a micropolarizer array illuminated with (a) polarized light and (b) nonpolarized light. It was fabricated using the SFIL process described in Fig. 3(B) (steps 1–5) followed by metal liftoff. (c) SEM image of the micropolarizer's metal lines.

The ultimate goal of the collaboration was to pattern a nonflat substrate with imprint lithography. Starting with a prepatterned substrate, typically a silicon wafer with either a Fresnel lens or hologram etched 700 nm deep into silicon, 497 000 molecular weight PMMA was spun on at 6000 rpm to provide a thin organic soluble layer with which to perform metal liftoff in an acetone ultrasonic bath. Then, a planarization layer of pure organic solution was photopolymerized over the hard-baked PMMA. Finally, the etch barrier was patterned over the organic planarized layer. High-aspect-ratio resist features such as those shown in Figs. 16(a) and 16(b) were generated using the same etch transfer process as that used for flat substrates. Features as small as 250 nm were etched over the 700 nm topography. After patterning these substrates using SFIL, 50 nm of Ti was deposited exactly the

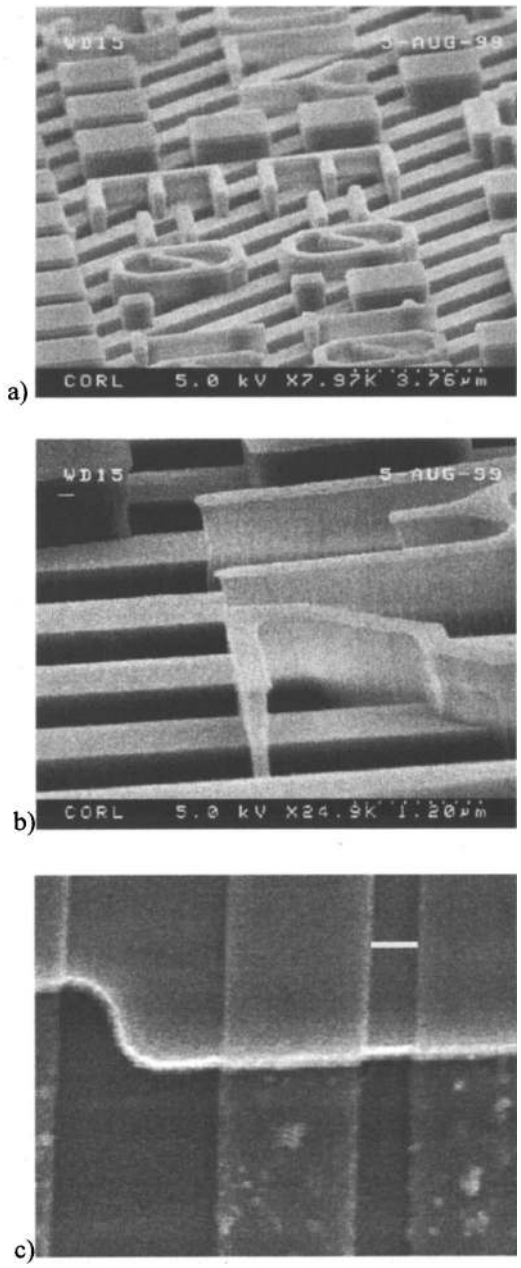

FIG. 16. (a) 2 μm and smaller features patterned over 700 nm topography; (b) 250 nm feature transferred through the organic layer and topography like that in (a); (c) metal lines patterned over 700 nm topography using SFIL and metal liftoff.

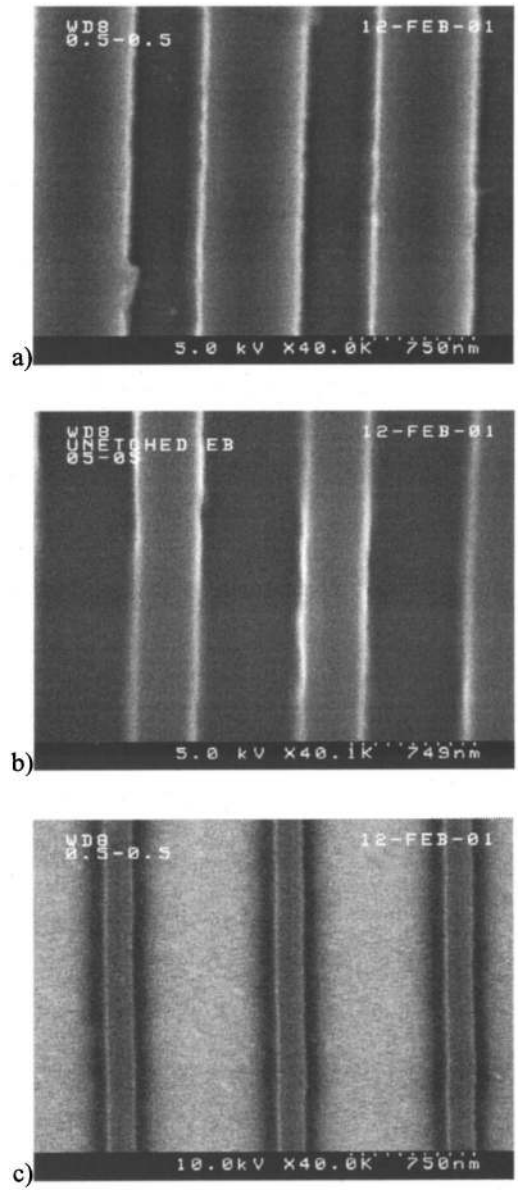

FIG. 17. Top-down SEM image of (a) a quartz template having 600 and 400 nm line spaces; (b) of features replicated in the SFIL etch barrier; (c) of features etch transferred through the transfer layer.

same as for the high-resolution lines. Metal liftoff was performed in an acetone ultrasonic bath. These results are shown in Fig. 16(c). There is no measurable change in the linewidth from the top of the 700 nm topography to the bottom.

A template fabricated at IBM–Burlington was used to demonstrate the RIE process on substrates patterned on the multi-imprint stepper that utilizes a rigid quartz template. The template was characterized at IBM–Burlington for line–space dimensions. A comparison of the line spaces of the template to those of the replicated features, and of the transferred image is shown in Fig. 17. There is no detectable difference in the line–space widths between the template and the replicated features; however, there is significant bias between the linewidths of the replicated features and the etched images. The etch process must be further optimized to minimize this bias. Figure 18 shows a series of SEM images that provide details of the sidewall smoothness achieved. Further evaluation of the feature biasing caused by RIE and by the photopolymerization is being investigated.

VI. CONCLUSIONS

Step and flash imprint lithography is capable of high-resolution patterning at room temperature with less than 14 N applied force. Separation occurs at less than 35 kPa. SFIL successfully utilizes commercially available chemicals to pattern in the sub-100 nm regime. A rigid template readily

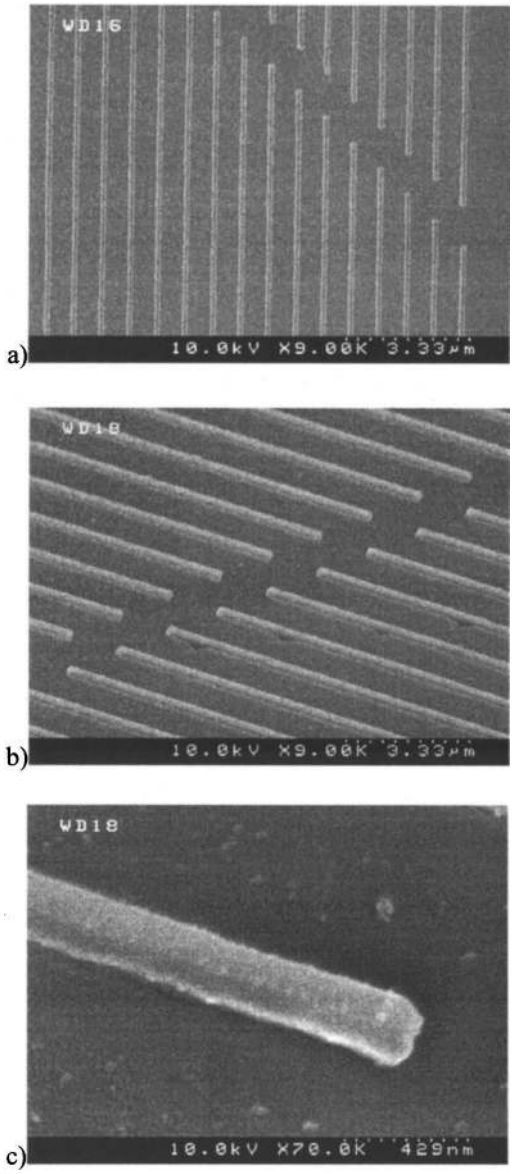

FIG. 18. SEM images of features patterned with a rigid template and etched through the transfer layer. (a) Large area top-down view; (b) 60° tilt; and (c) high resolution image of the 60° tilt edge.

displaces its low viscosity etch barrier formulation with 12 kPa resulting in 138 nm base layers. The completion of the SFIL stepper marks the first step toward imprint lithography and the possibility of high-resolution layer-to-layer alignment. The first features replicated with the SFIL stepper have been successfully etched through the transfer layer. The step and flash multilayer scheme was successfully applied to the patterning of 60 nm lines with 6:1 aspect ratios and of 80 nm features with 14:1 aspect ratios. Using metal liftoff we have successfully patterned 100 nm metal L/S and generated a micropolarizer array. Exploiting the high-aspect-ratio patterning of SFIL's multilayer scheme, 250 nm features were patterned over the 700 nm topography. After the Ti lift-off process, the metal lines exhibit no measurable change in feature size from top to bottom of the 700 nm deep topography.

ACKNOWLEDGMENTS

The authors would like to thank all those at Agilent Laboratories for all their assistance especially Judith Seeger, Karen Seaward, and Jim Krugger (currently at IBM). They appreciate the donations and technical support from IBM, ETEC, Ultratech Stepper, and 3M. The would also like to thank DARPA (MDA972-97-1-0010) and SRC (96-LC-460) for their continued support of the SFIL research.

[1]3rd International SEMATECH Next Generation Lithography Workshop, Colorado Springs, CO, 6–9 December 1999.
[2]M. J. Bowden, L. F. Thompson, and C. G. Willson, *Introduction to Microlithography* (American Chemical Society, Washington, DC, 1994).
[3]M. Colburn *et al.*, Proc. SPIE **3676**, 379 (1999).
[4]M. Colburn, A. Grot, M. N. Amistoso, B. J. Choi, T. C. Bailey, J. G. Ekerdt, S. V. Sreenivasan, J. Hollenhorst, and C. G. Willson, Proc. SPIE **3997**, 453 (2000).
[5]S. Y. Chou, P. R. Krauss, and P. R. Renstrom, J. Vac. Sci. Technol. B **14**, 4129 (1996).
[6]Y. Xia and G. M. Whitesides, Angew. Chem. Int. Ed. Engl. **37**, 550 (1998).
[7]J. Haisma, M. Verheijen, K. van der Huevel, and J. van den Berg, J. Vac. Sci. Technol. B **14**, 4124 (1996).
[8]R. W. Jaszewski, H. Schift, J. Gobrecht, and P. Smith, Microelectron. Eng. **41/42**, 575 (1998).
[9]H. Schulz *et al.*, J. Vac. Sci. Technol. B **18**, 1861 (2000).
[10]H.-C. Scheer, H. Schults, F. Gottschalch, T. Hoffmann, and C. M. Sotomayor Torres, J. Vac. Sci. Technol. B **16**, 3917 (1998).
[11]J. Shaw, E. Babich, M. Hatzakis, and J. Paraszczak, Solid State Technol. **30**, 83 (1987).
[12]G. Bouwhuis, J. Braat, A. Huijser, J. Pasman, G. van Rosmalen, and K. S. Immink, *Principles of Optical Disc Systems* (Hilger, Bristol, UK, 1985).
[13]P. Ruchhoeft *et al.*, J. Vac. Sci. Technol. B **17**, 2965 (1999).
[14]M. Colburn, Ph.D. thesis, The University of Texas at Austin, Austin, TX, 2001.
[15]T. Bailey, B. J. Choi, M. Colburn, A. Grot, M. Meissl, S. Shaya, J. G. Ekderdt, S. V. Sreenivasan, and C. G. Willson, J. Vac. Sci. Technol. B **18**, 3572 (2000).
[16]B. J. Choi, S. Johnson, S. V. Sreenivasan, M. Colburn, T. Bailey, and C. G. Willson, ASME DETC 2000/MECH 14140, Baltimore, MD, 2000.
[17]S. Smith and D. G. Chetwynd, *Foundations of Ultraprecision Mechanism Design* (Gordon and Breach Science, Philadelphia, 1992).
[18]Summers Optical, a division of EMS Acquisition Corp., 321 Morris Rd., P.O. Box 162, Fort Washington, PA 19034.